Journal of Catalysis 319 (2014) 194–199

Contents lists available at ScienceDirect

Journal of Catalysis

journal homepage: www.elsevier.com/locate/jcat

# Understanding promotion of photocatalytic activity of $TiO_2$ by Au nanoparticles

Rezvaneh Amrollahi [a,b], Mohamed S. Hamdy [a,c], Guido Mul [a,*]

[a] Photocatalytic Synthesis (PCS) Group, MESA+ Institute for Nanotechnology, Faculty of Science and Technology, University of Twente, The Netherlands
[b] Department of Physics, Iran University of Science and Technology, Tehran, Iran
[c] Chemistry Department, Faculty of Science, Helwan University, Cairo, Egypt

ARTICLE INFO

*Article history:*
Received 20 May 2014
Revised 24 August 2014
Accepted 27 August 2014
Available online 29 September 2014

*Keywords:*
Au
$TiO_2$
Photocatalysis
Selective oxidation
Wavelength
Plasmon resonance energy transfer (PRET)
Hot electrons

ABSTRACT

Au nanoparticles prepared by deposition–precipitation were evaluated in promoting photocatalytic activity of $TiO_2$ (P25) in the oxidation of methylcyclohexane. At 375 nm and in particular at 425 nm, Au was found to significantly enhance the rate induced by P25. Illumination of Au-promoted P25 at 525 nm did not result in any measureable activity. To validate whether the enhancement at 425 nm is purely catalytic, or if plasmonic effects are relevant, we compared the rates of Au/$TiO_2$ with Pt-promoted $TiO_2$ at 375 and 425 nm. At 375 nm, Pt nanoparticles induced larger catalytic effects than Au nanoparticles, whereas the rate enhancement induced by Pt was much lower than of Au at 425 nm. We assign the thus demonstrated Au based plasmonic phenomena at 425 nm to the so-called plasmon resonance energy transfer, rather than to hot electron transfer, given the absence of activity at 525 nm.



## 1. Introduction

$TiO_2$ is by far the most studied metal oxide photocatalyst, and many ways of manipulating the bulk and surface composition have been reported in the literature to enhance the activity [1–5]. Modifications are generally aimed at improving light absorption over a large range of (visible) wavelengths, as well as promoting electron–hole separation and transfer efficiency by e.g. annealing and addition of metal-, and/or metal oxide nanoparticles [6,7]. Recently, intriguing studies have been reported on an additional method to promote activity of (doped) $TiO_2$, i.e. the use of plasmon absorption properties of metal nanoparticles of typically Ag or Au [8–10]. Enhanced activity by incorporation of plasmonic particles in photocatalytically active layers has been reported for various reactions, including (gas phase) oxidation reactions of organic molecules [11] and (liquid phase) water splitting [12–14]. Two phenomena have been proposed in explaining the rate enhancement by plasmonic (nano) particles. (i) Photo-excitation of Au nanoparticles leads to a quasi electron–hole pair, of which the electron can be transferred to the conduction band of $TiO_2$ and subsequently to a reactant (in this case oxygen), and the hole induces oxidation reactions on Au adsorbed species [15–19], and (ii) plasmon excitation by absorption of a photon corresponding to the plasmon absorption band, results in an energy field (plasmon resonance energy) which positively influences $TiO_2$ excitation by absorption of a second photon, of larger energy than the band gap (in the case of $TiO_2$). This phenomenon is predominantly observed if overlap exists between plasmon and band-gap absorption [9,20–23].

In this study, we address the possible plasmonic effect of Au nanoparticles prepared by deposition–precipitation on the photocatalytic activity of $TiO_2$ in a liquid phase hydrocarbon oxidation reaction, i.e. the conversion of methylcyclohexane to methylcyclohexanone. Photocatalytic activity of Au/P25 was evaluated by *in situ* ATR-FTIR spectroscopy. We will demonstrate that of the wavelengths investigated (375, 425 and 525 nm, and combinations thereof), Au nanoparticles are only effective in promoting rates at 375 and 425 nm. Furthermore, by comparing the promotion in rate induced by Au nanoparticles and Pt nanoparticles at these two wavelengths, we demonstrate that besides a catalytic effect, a plasmonic enhancement induced by Au is apparent, which is most likely associated with plasmon resonance energy transfer, rather than electron transfer.

## 2. Experimental section

### 2.1. Catalysts and chemicals

P25 was obtained from Evonik, while $HAuCl_4$ and Methylcyclohexane (MCH) were purchased from Sigma–Aldrich. P25, $HAuCl_4$

* Corresponding author. Fax: +31 53 4892882.
*E-mail address:* g.mul@utwente.nl (G. Mul).

http://dx.doi.org/10.1016/j.jcat.2014.08.017
0021-9517/

and MCH were used as received without further purification. The Pt promoted P25 catalyst was prepared by atomic layer deposition and kindly provided by the Delft University of Technology. Details of the methodology of atomic layer deposition and the morphology and characteristics of the Pt catalyst can be found in [24]. The loading of Pt was the same as in Au the catalyst, i.e. 0.2 wt%, while the average particle size was smaller, in the order of 5–6 nm.

### 2.2. Preparation of the Au/P25 catalyst

Gold was deposited on the P25 surface at 0.2 wt% loading by deposition–precipitation. In this procedure, 0.3 g of $TiO_2$ P25 was added to an aqueous solution of $HAuCl_4$ (0.1 M) previously adjusted to pH 9 by drop-wise addition of NaOH (0.1 M). The slurry was maintained at room temperature, and vigorously stirred overnight. Subsequently, the sample was filtered, washed with deionized water to remove chlorides, and then dried at 80 °C for 4 h in a furnace (static air). Finally, the obtained purple powder was calcined at 450 °C (heating rate 10 K/min) in static air for 5 h. To exclude the influence of preparative conditions on the behavior of P25 in the photocatalytic reaction [25], all preparative steps were performed for P25 in the absence of the Au solution (0.1 M HCl was used instead), and this sample is denoted as calcined P25 throughout the manuscript. To allow ATR analysis of methylcyclohexane oxidation, the catalysts were suspended in water at a concentration of 3 g/L. These suspensions were treated for 30 min in a 35 kHz Elmasonic ultrasonic bath; 2 mL of the resulting mixture was spread on a ZnSe crystal, followed by drying in vacuum overnight.

### 2.3. Material characterization

The crystal structure of the material was determined by powder X-ray diffraction (XRD), using a Philips PW2050 diffractometer with Cu Kα radiation ($\lambda = 0.15406$ nm). Measurements were recorded in steps of 0.005° with a count time of 1 s in the $2\theta$ range of 20° and 80°. Raman spectroscopy was performed at room temperature using a Raman spectrometer (Bruker Senterra) with a green laser 532 nm (2 mW). Spectra were acquired at a resolution of ~15 $cm^{-1}$, and 10 scans were accumulated for each spectrum. The BET area was measured by nitrogen adsorption at liquid nitrogen temperature in a Micrometrics ASAP 2400 apparatus. Before analysis, the samples were degassed for 24 h at 300 °C in vacuum. Diffuse reflectance UV–vis spectra (DRS) of the powders were recorded at ambient pressure and temperature on a Thermo Scientific Evolution 600 spectrophotometer, equipped with a diffuse reflectance accessory of Harrick, using $BaSO_4$ as reference. Spectra were recorded in the wavelength range of 350–800 nm. TEM imaging was carried out using a Philips CM300ST-FEG microscope equipped with a Kevex EDX detector. Samples for TEM were prepared by deposition of a dispersion in ethanol onto a carbon coated TEM grid.

### 2.4. Photo-oxidation of methylcyclohexane

The photocatalytic activity was determined using an attenuated total reflectance–Fourier transform infrared (ATR–FTIR) setup (Bruker Vertex 70 spectrometer, equipped with a Harrick Scientific ATR accessory). The ZnSe crystal coated with the catalyst formulation was inserted in the sampling compartment of the spectrometer. 20 mL of MCH was saturated with $O_2$ by bubbling dry air at 8 mL/min for 30 min. Subsequently, $O_2$ saturated MCH was added to the catalyst layer, and the composition enclosed by a top plate containing a quartz window. Prior to the photocatalytic oxidation experiments, adsorption of MCH on the catalyst coating was monitored for 100 min. Then, a spectrum of adsorbed MCH on the coating was collected, and used as background spectrum for photocatalysis experiments. To study the effect of multiple wavelengths on photocatalytic activity, an assembly of 7 LEDs was used as light source. We used two different LED arrays. Both have 3 LEDs emitting at 525 nm, one alternating with four 375 nm LEDs, and another alternating with four 425 nm LEDs. The LEDs of different wavelengths could be switched on and off independently. The light intensity of the LEDs was fine-tuned to be equal at 1.5 mW/$cm^2$. A scheme of the ATR–FTIR setup is shown in the Supporting Information (Fig. S1). Upon illumination, each spectrum was recorded at fixed time intervals (typically 1 min) from 4000 to 700 $cm^{-1}$ by collecting 64 scans with a resolution of 1.5 $cm^{-1}$.

## 3. Results

### 3.1. Characterization

Fig. 1 shows TEM images of the Au/$TiO_2$ sample prepared by the deposition–precipitation method (DP). Based on these images and energy-dispersive X-ray (EDX) analysis, Au nanoparticles are clearly identified ranging in size between 10 and 20 nm. Further, these results indicate that the deposition precipitation method did not induce changes in $TiO_2$ morphology, of which the mean primary particle size is estimated to be around 15 nm. The Au particle size obtained in this study is a bit larger than usually reported. This is likely because of the sensitivity of the Au particle size on synthesis procedure, such as Au source, stirring rate, pH, calcination temperature and ramp rate of calcination. XRD and Raman analysis confirm the absence of dramatic changes in crystallinity and size of P25 $TiO_2$, potentially induced by the solutions used for Au deposition, and/or calcination (Figs. S2 and S3). The lower intensities of the Raman features of P25 after Au deposition are likely the result

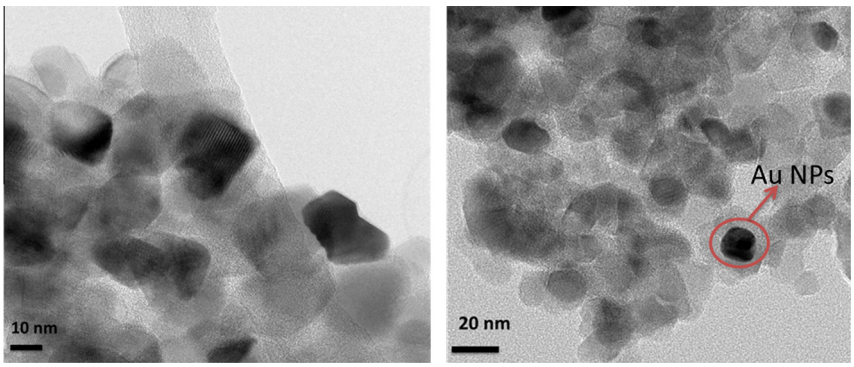


**Fig. 1.** Transmission electron microscopy (TEM) images of Au/p25 (0.2%).

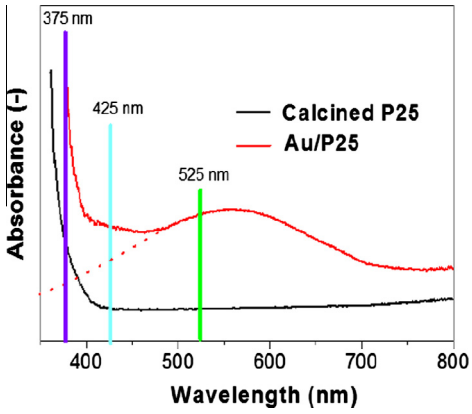


**Fig. 2.** UV–vis diffuse reflectance spectra of Au/P25 and P25 both calcined at 450 °C for 5 h.

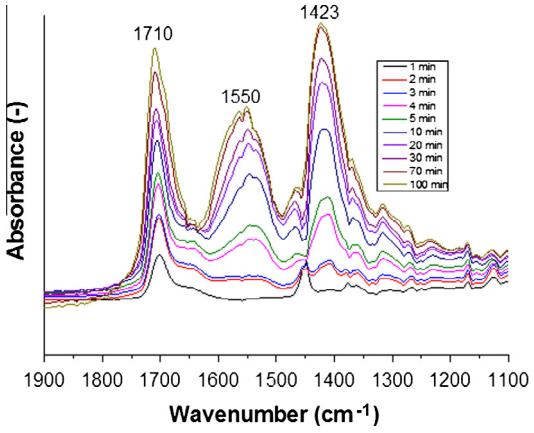


**Fig. 3.** ATR–FTIR spectra of MCH on Au/P25 after illumination at 375 nm recorded from 1 min to 100 min.

of absorption of the laser light by the Au particles used for analysis (532 nm), reducing the scattering efficiency.

The diffuse reflectance UV–vis spectra of $TiO_2$ and Au/P25 were recorded in the range of 350–800 nm, and the results are shown in Fig. 2. P25 has no significant absorptions in the visible region (band edge at around 410 nm), while the surface plasmon absorption of gold nanoparticles can be observed maximizing around 560 nm.

### 3.2. Photoactivity of Au/P25 as a function of wavelength of excitation

The spectrum of MCH on Au/P25 after it had been exposed to illumination at 375 nm for 100 min is presented in Fig. 3. After illumination, a broad range of infrared absorptions develop in time between 1800 $cm^{-1}$ and 1200 $cm^{-1}$. As described in a previous study [26], photocatalytic oxidation of MCH takes place via the formation of 2-methylcyclohexanone and/or 4-methylcyclohexanone by the oxidation of the cyclohexane ring. Subsequently, ring opening and formation of several carboxylate species is apparent, in agreement with a study reported by Hernandez-Alonso et al. [27]. To validate the rate of reaction induced by the various catalytic formulations, we show the rate of development of the intensity of the ketone band at 1710 $cm^{-1}$ as a function time (Fig. 4), particularly focusing on the initial growth rate: consecutive oxidation leads to irreversibly adsorbed carbonates and carboxylates, which severely deteriorates the catalytic performance (as can be clearly observed in all the curves, as *per* the leveling off to a more or less constant product concentration). Fig. 4 shows the curves derived from the spectral data for P25 at 375 and 425 nm, in the absence or presence of Au nanoparticles.

At 375 nm (Fig. 4a), both catalysts show a similar initial rate, while the growth of the ketone band continues for a longer period of time for the Au containing catalyst. This can be explained on the basis of Scheme 1: the rate of decomposition of carboxylates and carbonates to gas phase $CO_2$ ($k_3$) is likely higher in the presence of Au, causing the surface to be less quickly saturated with these species, thus maintaining high photocatalytic MCH oxidation activity (Scheme 1). This explanation is corroborated by literature data [28], showing smaller intensities of carboxylate and carbonate bands in the presence of Au, and the observation of large positive bands in the IR spectra of the Au containing catalyst in the present study in the region of spectral features of (adsorbed) water, the co-product of total oxidation of MCH to $CO_2$. In addition, in the Supplementary information (Fig. S4), we show ATR–FTIR spectra obtained after oxidation of MCH at 375 nm for 100 min for Au/P25 and P25, respectively. The absorption intensity of (dissolved) $CO_2$ is significantly higher for the Au containing catalyst, confirming a larger degree of complete oxidation induced by the presence of Au.

The comparison of the rates of ketone formation at 425 nm in the absence or presence of Au is shown in Fig. 4b. Now the difference in initial rate is significant as compared to illumination at 375 nm. The initial rate for calcined P25 is 8 times smaller than for Au/P25 under the same reaction conditions. At the two wavelengths of excitation, the steady state (surface) composition of

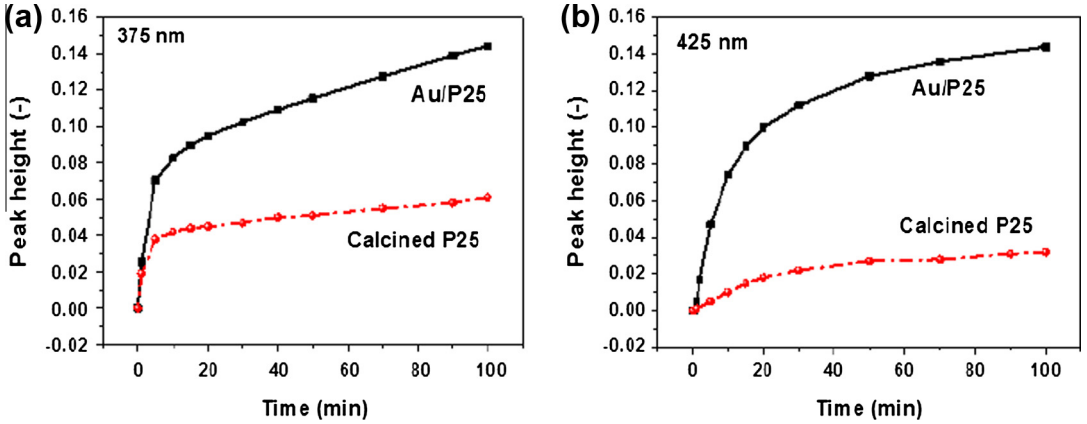


**Fig. 4.** The time evolution of the peak height of the ketone vibrations (1710 $cm^{-1}$) for both calcined P25 and Au/P25, respectively, induced by photocatalytic oxidation of MCH at 375 nm (a) and 425 nm (b).

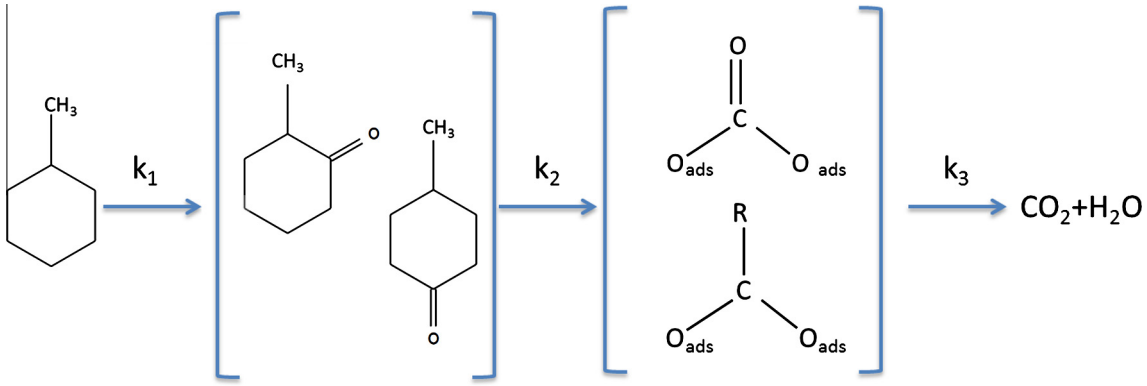


**Scheme 1.** Pathways of photocatalytic oxidation of MCH in the liquid phase. The rate of ketone formation ($k_1$), the rate of consecutive oxidation ($k_2$), and the rate of decomposition of carboxylates and carbonates to gas phase $CO_2$ ($k_3$) are indicated.

the Au containing catalyst is similar, showing higher quantity of ketone as compared to P25.

When both catalysts were excited at 525 nm (Fig. 5), no appreciable rate of reaction was observed. This result is in agreement with earlier studies, which also did not show any activity in the conversion of cyclohexane over Au promoted $TiO_2$ when illuminated at 525 nm [28].

### 3.3. Multiple wavelength excitation

Various experiments were conducted at multiple wavelength excitation (see scheme Fig. 5). In Fig. 5, experiment numbers 1 and 4 are showing the previously discussed results of illumination by 375 and 525 nm independently. When the Au containing samples were illuminated with 375 (UV light) and 525 nm simultaneously (either with a delay (experiment 2), or without a delay (experiment 3)), no appreciable enhancement of the rate in methylcyclohexanone formation (again derived from spectral growth at 1710 $cm^{-1}$) was observed. On the contrary, co-excitation of Au nanoparticles at 525 nm slightly reduces the activity, while also the maximum attainable ketone concentration seems to be lowered. The slightly negative effect in rate by co-excitation with 525 nm light suggests potential heating of the Au particles is not contributing to enhancing the rate of P25 at 375 nm [29]. On the contrary, the higher expected local temperature of the Au particles likely reduces the amount of adsorbed oxygen, needed for affective electron transfer and thus photocatalysis.

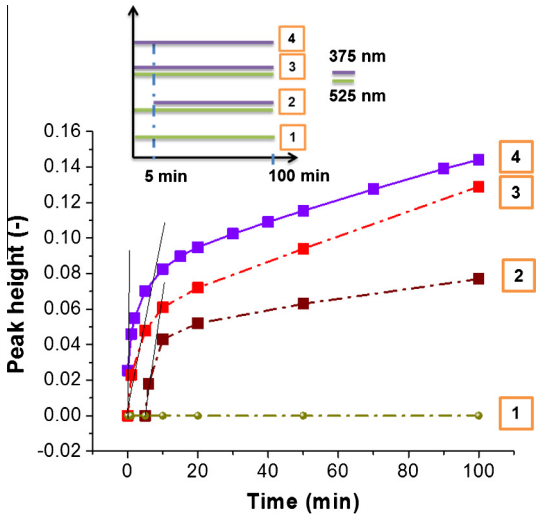


**Fig. 5.** The time evaluation of the peak height of the ketone (1712 $cm^{-1}$) vibration for Au/P25, induced by photocatalytic oxidation of MCH. (1) Just 525 nm, (2) 375 nm and 5 min later 525 nm, (3) Both 375 and 525 nm at the same time, and (4) 375 nm only.

The photooxidation of methylcyclohexanone over Au/P25 was also measured for a combination of 425 nm and 525 nm (Fig. 6). Again, addition of light energy at 525 nm, exciting the Au NPs, slightly reduces activity. In Fig. 6b the selectivity, determined by dividing the peak height at 1710 nm (ketone) over 1552 nm (carboxylate) during the reaction, is displayed. As expected, the selectivity decreases as a function of time of reaction. The rate at which selectivity decreases is similar in the absence or the presence of 525 nm light.

### 3.4. Comparison of Au and Pt nanoparticles

To validate whether the enhancement at 425 nm is purely catalytic, or if plasmonic effects are relevant, we compared the rates of $Au/TiO_2$ with Pt-promoted $TiO_2$ (0.2 wt.% loading, with average particle size of Pt in the range of 5–6 nm) at 375 and 425 nm (Fig. 7). At 375 nm, Pt nanoparticles induced a similar initial rate of reaction as compared to Au nanoparticles, but the time at which leveling off in the growth of the ketone band is observed is significantly longer. This can be explained by the high catalytic efficiency of Pt in the oxygen reduction reaction; an essential half reaction in converting alkanes over photo-excited $TiO_2$ either to selective products and/or $CO_2$. We suggest the latter is relevant for maintaining the observed catalytic activity over an extended period of time. Surprisingly, the effect of Pt nanoparticles was much less significant than of the Au nanoparticles in the reaction performed at 425 nm, both in terms of initial rate, and in maximized attainable (surface) ketone quantity. Fig. 7b also shows a comparison between commercial P25, calcined P25 at 450 °C, and calcined P25 following the liquid exposures relevant for the applied deposition–precipitation method. The spectral data show different treatments of P25 do not have a significant effect on photocatalytic activity in the oxidation of methyl cyclohexane, and therefore likely do not significantly contribute to the identified changes related to metal deposition. At the same time, these data show that P25 is active at this relatively long wavelength, indicating light absorption is feasible. The comparison of reaction rates strongly suggests the effect of Au at 425 nm is not only catalytic, but also plasmonic, of which the mechanism is discussed in the following.

## 4. Discussion

Before discussion of the data of activation at 425 nm, the observed effects at 375 nm are addressed. Principally, the improve-

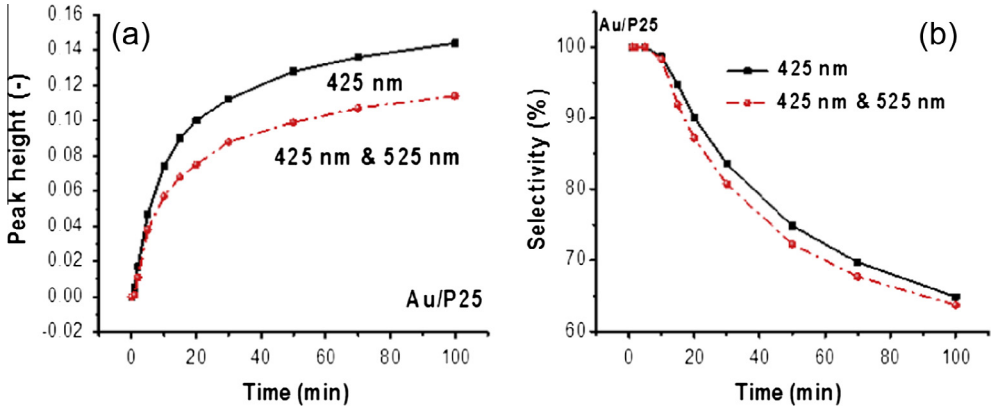


**Fig. 6.** Catalytic rates (a) and selectivity changes (b) observed at 425 nm as compared to illumination with 425 nm and 525 nm simultaneously.

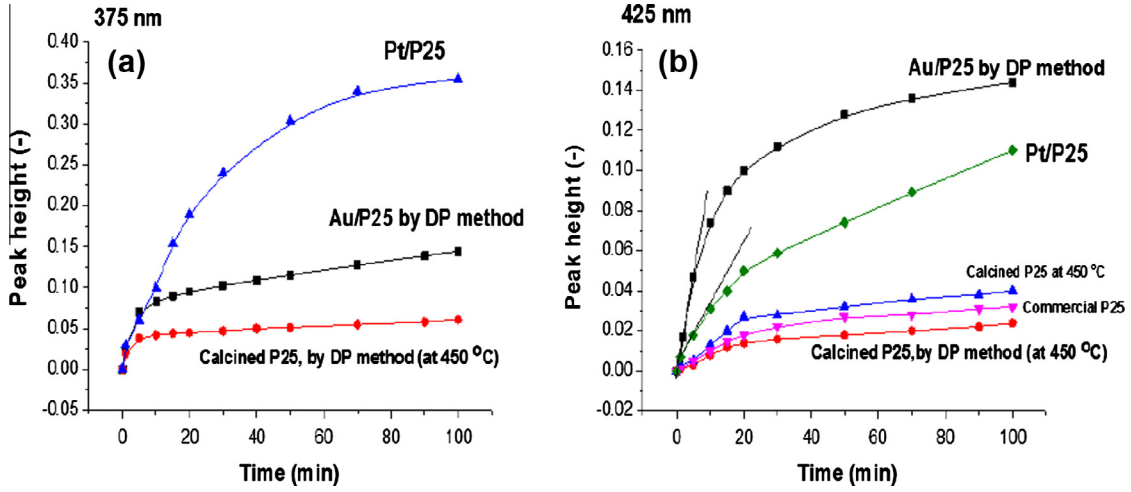


**Fig. 7.** The time evolution of the peak height of the Ketone (1710 $cm^{-1}$) vibration for calcined P25, Au/P25 and Pt/P25, respectively, induced by photocatalytic oxidation of MCH at 375 nm (a) and calcined P25 at 450 °C, commercial P25, calcined P25, Au/P25, and Pt/P25, respectively, at 425 nm (b).

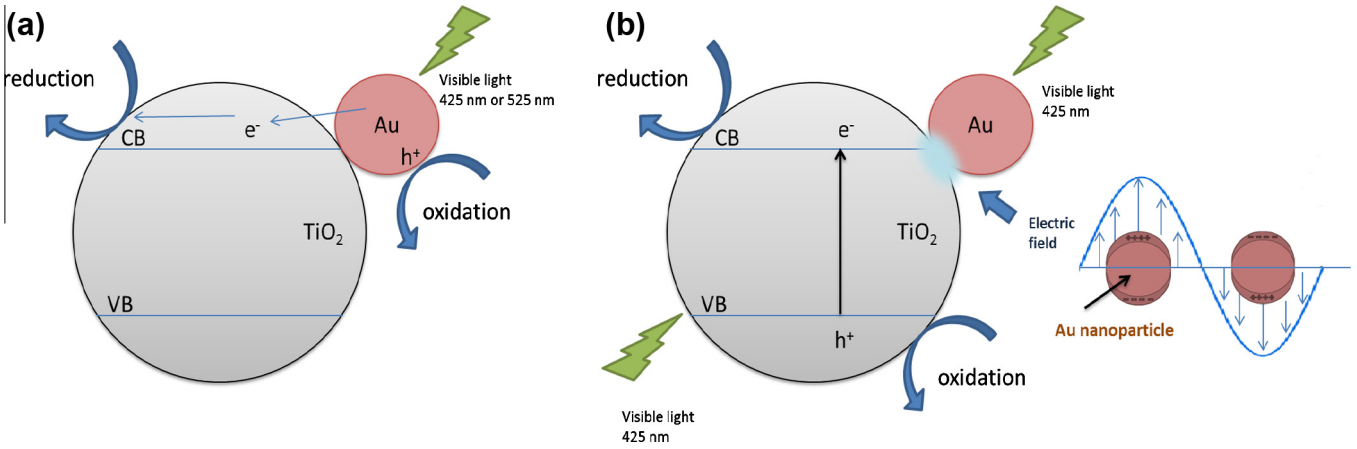


**Fig. 8.** Illustration of the mechanism of 'hot electron transfer' proposed by [10,19] (a), and of plasmon energy transfer proposed by [9,20] (b).

ment in catalytic behavior imposed by the Au and Pt nanoparticles at these wavelengths can be explained by the commonly advocated mechanism in which electron transfer from $TiO_2$ to the metallic NPs occurs, which has been demonstrated to be energetically favorable [29]. Further, the NPs catalyze oxygen reduction, (Pt more efficiently than Au), hence explaining the observed phenomena in Fig. 7.

On the other hand, the promoting effect of Au NPs at 425 nm is likely not purely catalytic, since compared to Pt (an excellent oxygen reduction catalyst), the effect of Au is much more significant, whereas the better catalytic properties of Pt are apparent at 375 nm. In order to explain the data obtained by illumination at 425 nm, we summarize the two plasmon absorption-related mech-

anisms that have been reported in the literature: (i) Photo-excitation of Au nanoparticles leads to an electron–hole pair, of which the electron can be transferred to the conduction band of $TiO_2$, and the hole induces oxidation reactions [15–19]. In 2004, Tatsuma's group proposed this charge transfer mechanism to explain their observation of photon to current conversion efficiency (IPCE) of $TiO_2$ increasing upon functionalization with Au or Ag [19]. Several groups used this mechanism to explain the effect of Au or Ag nanoparticles in promoting visible light induced photocatalytic reactions, such as water splitting [10], decomposition of methyl orange [30], and photooxidation of organic compounds [31]. (ii) Plasmon excitation results in an energy field (plasmon resonance energy) which positively influences $TiO_2$ excitation. This phenomenon is predominantly observed if overlap exists between plasmon and band-gap absorption [9,22,23,29]. Both mechanisms are illustrated in Fig. 8a and b, respectively. The results of the present study support the second explanation of the promoting effect of Au, since excitation of Au nanoparticles at 525 nm did not result in any observable rate in catalysis of alkane activation. Apparently charge transfer of the electrons to the conduction band of $TiO_2$ is not feasible under our reaction conditions. This might be related to the relatively large particle size (~10–20 nm) of the Au particles in the present study: the mean free path of electrons in metal particles is in the order of 1–2 nm, and hence, photoexcited electrons have a low probability to 'escape' a 10–20 nm sized particle. A recent study by Chakarov et al. confirms the absence of catalytic conversion of $TiO_2$ functionalized with relatively large Au particles by excitation at 525 nm [29]. Overlap between the absorption of P25 and Au nanoparticles is apparently necessary to induce a synergistic effect, and present at 425 nm (Fig. 2, light absorption of P25 at 425 nm demonstrated affective for photocatalysis by data in Fig. 7), although admittedly relatively small. The observed activity in the present study is in agreement with recent studies advocating plasmon resonance energy transfer as an important phenomenon for plasmon induced photocatalysis [9,29], which studies provide significant additional physical background.

## 5. Conclusions

We performed selective oxidation of MCH over P25 in the presence or absence of Au nanoparticles and demonstrate for the first time that 10 nm Au particles have a strong positive effect on the photocatalytic rate in selective alkane oxidation of P25 upon illumination (with a 20 nm band width centered) at 425 nm: a wavelength allowing simultaneous photoexcitation of the P25 catalyst and Au nanoparticles. The effect is corroborated by the much stronger positive effect of Au at 425 nm, as compared to induced by Pt nanoparticles, excluding catalytic effects to be dominant. Since excitation at 525 nm does not lead to any activity for the studied reaction, we assign the plasmonic effect to the so-called plasmon energy transfer mechanism, requiring spectral overlap of band gap and plasmon absorption, rather than to the 'hot electron injection' theory.

## Acknowledgments

R. Amrollahi thank the Ministry of Science, Research and Technology of the Islamic Republic of Iran for her personal scholarship. A. Goulas and J.R. van Ommen (Delft University of Technology) are kindly acknowledged for providing the Pt-promoted P25 catalyst. D. Chakarov (Chalmers University, Sweden), and H. Garcia (Universidad Politécnica de Valencia, Spain) are kindly acknowledged for fruitful discussions.

## Appendix A. Supplementary material

Supplementary data associated with this article can be found, in the online version, at http://dx.doi.org/10.1016/j.jcat.2014.08.017.

## References

[1] I. Paramasivam, J.M. Macak, P. Schmuki, Electrochem. Commun. 10 (2008) 71–75.
[2] H. Zhang, X. Lv, Y. Li, Y. Wang, J. Li, ACS Nano 4 (2010) 380–386.
[3] J. Yu, Q. Xiang, M. Zhou, Appl. Catal. B: Environ. 90 (2009) 595–602.
[4] S.G. Kumar, L.G. Devi, J. Phys. Chem. A 115 (2011) 13211–13241.
[5] M.A. Henderson, Surf. Sci. Rep. 66 (2011) 185–297.
[6] A. Primo, A. Corma, H. Garcia, Phys. Chem. Chem. Phys. 13 (2011) 886–910.
[7] J.Y. Lan, X.M. Zhou, G. Liu, J.G. Yu, J.C. Zhang, L.J. Zhi, G.J. Nie, Nanoscale 3 (2011) 5161–5167.
[8] B.Z. Tian, J.L. Zhang, T.Z. Tong, F. Chen, Appl. Catal. B: Environ. 79 (2008) 394–401.
[9] S. Linic, P. Christopher, D.B. Ingram, Nat. Mater. 10 (2011) 911–921.
[10] C. Gomes Silva, R. Juarez, T. Marino, R. Molinari, H. Garcia, J. Am. Chem. Soc. 133 (2011) 595–602.
[11] D. Tsukamoto, Y. Shiraishi, Y. Sugano, S. Ichikawa, S. Tanaka, T. Hirai, J. Am. Chem. Soc. 134 (2012) 6309–6315.
[12] R. Abe, J. Photoch. Photobio. C 11 (2010) 179–209.
[13] O. Rosseler, M.V. Shankar, M.K.L. Du, L. Schmidlin, N. Keller, V. Keller, J. Catal. 269 (2010) 179–190.
[14] J.J. Chen, J.C.S. Wu, P.C. Wu, D.P. Tsai, J. Phys. Chem. C 115 (2011) 210–216.
[15] W.-T. Chen, Y.-J. Hsu, P.V. Kamat, J. Phys. Chem. Lett. 3 (2012) 2493–2499.
[16] K. Adachi, K. Ohta, T. Mizuno, Sol. Energy 53 (1994) 187–190.
[17] Y. Tian, T. Tatsuma, J. Am. Chem. Soc. 127 (2005) 7632–7637.
[18] M.S. Devadas, K. Kwak, J.-W. Park, J.-H. Choi, C.-H. Jun, E. Sinn, G. Ramakrishna, D. Lee, J. Phys. Chem. Lett. 1 (2010) 1497–1503.
[19] Y. Tian, T. Tatsuma, Chem. Commun. (2004) 1810–1811.
[20] D.B. Ingram, P. Christopher, J.L. Bauer, S. Linic, ACS Catal. 1 (2011) 1441–1447.
[21] Y. Lu, H.T. Yu, S. Chen, X. Quan, H.M. Zhao, Environ. Sci. Technol. 46 (2012) 1724–1730.
[22] S.L. Zou, G.C. Schatz, Chem. Phys. Letts. 403 (2005) 62–67.
[23] F. Le, D.W. Brandl, Y.A. Urzhumov, H. Wang, J. Kundu, N.J. Halas, J. Aizpurua, P. Nordlander, ACS Nano 2 (2008) 707–718.
[24] A. Goulas, J.R. van Ommen, J. Mater. Chem. A 1 (2013) 4647–4650.
[25] J.T. Carneiro, C.C. Yang, J.A. Moma, J.A. Moulijn, G. Mul, Catal. Lett. 129 (2009) 12–19.
[26] M.S. Hamdy, R. Amrollahi, G. Mul, ACS Catal. 2 (2012) 2641–2647.
[27] M.D. Hernandez-Alonso, I. Tejedor-Tejedor, J.M. Coronado, M.A. Anderson, Appl. Catal. B: Environ. 101 (2011) 283–293.
[28] J.T. Carneiro, T.J. Savenije, J.A. Moulijn, G. Mul, J. Photoch. Photobio. A 217 (2011) 326–332.
[29] R. Sellappan, M.G. Nielsen, F. Gonzalez-Posada, P.C.K. Vesborg, I. Chorkendorff, D. Chakarov, J. Catal. 307 (2013) 214–221.
[30] J. Yu, G. Dai, B. Huang, J. Phys. Chem. C 113 (2009) 16394–16401.
[31] J.W. Tang, ChemSusChem 3 (2010) 800–801.